

# Simultaneous Softening of $\sigma$ and $\rho$ Mesons associated with Chiral Restoration

K. Yokokawa<sup>(1)</sup>, T. Hatsuda<sup>(1)</sup>, A. Hayashigaki<sup>(1)</sup>, T. Kunihiro<sup>(2)</sup>

<sup>(1)</sup> *Department of Physics, University of Tokyo, Tokyo 113-0077 Japan and*

<sup>(2)</sup> *Yukawa Institute for Theoretical Physics, Kyoto University, Kyoto 606-8502, Japan*

(Dated: October 27, 2018)

Complex poles of the unitarized  $\pi$ - $\pi$  scattering amplitude in nuclear matter are studied. Partial restoration of chiral symmetry is modeled by the decrease of in-medium pion decay constant  $f_\pi^*$ . For large chiral restoration ( $f_\pi^*/f_\pi \ll 1$ ), 2nd sheet poles in the scalar ( $\sigma$ ) and the vector ( $\rho$ ) mesons are both dictated by the Lambert  $W$  function and show universal softening as  $f_\pi^*$  decreases. In-medium  $\pi$ - $\pi$  cross section receives substantial contribution from the soft mode and exhibits a large enhancement in low-energy region. Fate of this universality for small chiral restoration ( $f_\pi^*/f_\pi \sim 1$ ) is also discussed.

PACS numbers: 24.85.+p, 11.30.Rd, 13.75.Lb, 11.55.Fv

An analogy between in-medium hadrons in QCD and collective modes in condensed matters suggests that hadronic spectral functions and complex hadronic poles have important information on chiral structure of hot/dense matter [1]. In particular, the light vector mesons ( $\rho, \omega, \phi$ ) [2], and the light scalar meson ( $\sigma$ ) [3] have been proposed to be possible probes of partial restoration of chiral symmetry. Properties of in-medium vector mesons may be extracted through dilepton emission from hot and/or dense matter. In fact, relativistic heavy ion experiments in SPS at CERN indicate some spectral broadening and/or shift of the  $\rho$  [4, 5]. Dileptons observed in proton-nucleus reactions at KEK also suggest a low-mass spectral enhancement in the vector channel [6].

The  $\sigma$  meson, on the other hand, has been thought to be a direct but difficult probe of chiral restoration because of its obscure nature in the vacuum. Nevertheless, there arise growing interests in recent years to the  $\sigma$  in nuclear matter inspired by new experimental data of the  $\pi$ - $\pi$  invariant mass distribution in ( $\pi, \pi\pi$ ) [7, 8, 9] and ( $\gamma, \pi\pi$ ) [10] reactions with nuclear targets [11, 12]. They suggest some spectral change of the two-pion final states in the  $I=J=0$  channel ( $I$  and  $J$  being the total isospin and total angular momentum, respectively). Theoretically, the  $\sigma$  pole located deep in the complex energy plane may move toward the real-axis [3] and behave as an important precursory mode if the partial chiral restoration occurs [12, 13, 14].

The main aim of this paper is to investigate a common mechanism dictating the behavior of both  $\sigma$  and  $\rho$  when the partial chiral restoration takes place in nuclear matter. For this purpose, we study complex poles of the  $\pi$ - $\pi$  scattering amplitude in nuclear matter calculated in unitarized chiral models. To make reliable unitarization and analytic continuation of the scattering amplitude to complex energies, we adopt the  $N/D$  method [15, 16, 17] which respects the analyticity and approximately satisfies the crossing symmetry. As for the chiral models to be unitarized, we adopt four complementary models shown below. They are useful to check the model dependence of the final results.

*Model A:* The “ $\rho$  model” [18, 19] where  $\pi$  and bare- $\rho$  are the basic degrees of freedom. The physical  $\sigma$  is generated dynamically in this model.

*Model B:* The “ $\sigma$  model” [19, 20] where  $\pi$  and bare- $\sigma$  are the basic degrees of freedom. The physical  $\rho$  is generated dynamically in this model.

*Model C:* The “degenerate  $\rho$ - $\sigma$  model” [16] where  $\pi$ , bare- $\rho$  and bare- $\sigma$  are all basic degrees of freedom.

*Model D:* The leading order chiral lagrangian  $\mathcal{L}_2$ , by which the  $\sigma$ -pole is generated dynamically while the physical  $\rho$  is not [21].

To incorporate the effect of chiral symmetry restoration in these models, we replace the pion decay constant  $f_\pi$  by an in-medium decay constant  $f_\pi^*$  which is expected to decrease in nuclear matter [3]. In the  $\sigma$ -models, this replacement is approximately justified in the mean-field level where the effect of the Fermi-sea is absorbed in the redefinition of  $f_\pi$  [14]. In general, there arises two decay constants in the medium:  $f_{\pi,t}^*$  which is related to the temporal component of the axial current, and  $f_{\pi,s}^*$  which is related to the spatial component of the axial current. In the qualitative study given below, we will not consider this complication. For more discussions on  $f_\pi^*$ , see recent papers [22].

As for the parameters such as the masses of bare- $\rho$  and bare- $\sigma$  and their couplings to  $\pi$ , we keep them density independent, partly because it is a simplest possible choice and partly because their density dependence is not known. Nevertheless, we shall show that, in all the above models, there arise *simultaneous* softening of  $\sigma$  and  $\rho$  driven by the decrease of  $f_\pi^*$ . This is the first strong indication that both the scalar and vector mesons serve as chiral soft modes. To extract essential physics of the soft modes without complication due to the finite pion mass, we will work in the chiral limit below.

The  $\pi$ - $\pi$  scattering amplitude and associate phase shift in the vacuum ( $f_\pi=93$  MeV) in *Model C* has been studied in [16] by using the  $N/D$  method. We briefly recapitulate its essential parts which are necessary for the analyses in this paper. The invariant amplitude for the elastic process  $\pi^a + \pi^b \rightarrow \pi^c + \pi^d$  is written as  $\mathcal{M}_{abcd}(s, t) = A(s, t)\delta_{ab}\delta_{cd} +$  (crossing terms), where

$a, b, \dots$  denote isospin indices and  $s, t$  are the Mandelstam variables. The tree-level amplitude  $A^{\text{tree}}(s, t)$  is parameterized by the contact  $\pi\text{-}\pi$  interaction from  $\mathcal{L}_2$  together with the exchange of bare- $\sigma$  in the  $s$ -channel and the bare- $\rho$  exchange in  $t, u$ -channels [16]. Then the partial wave amplitude  $a_{IJ}$  has a general form

$$a_{IJ}^{\text{tree}}(s) = b_{IJ}s + \sum_{\alpha=\sigma,\rho} b'_{\alpha IJ} f_{\alpha}(s/\bar{m}_{\alpha}^2). \quad (1)$$

Here  $\bar{m}_{\sigma(\rho)}$  is the mass of the bare- $\sigma(-\rho)$ . The first term in the right hand side of eq.(1) is a *model-independent* part where  $b_{IJ}$  is the low energy constant solely determined by chiral symmetry;

$$b_{00} = \frac{1}{16\pi f_{\pi}^2}, \quad b_{20} = -\frac{1}{32\pi f_{\pi}^2}, \quad b_{11} = \frac{1}{96\pi f_{\pi}^2}. \quad (2)$$

The second term in (1) is a *model-dependent* part where the coefficient  $b'_{\alpha IJ}$  is proportional to  $g_{\alpha}^2$  with  $g_{\alpha}$  being a strength of the coupling of  $\alpha$  with two pions.  $f_{\alpha}(s/\bar{m}_{\alpha}^2)$  behaves as  $O(s^2)$  for  $s \rightarrow 0$ . We take  $\bar{m}_{\sigma}=\infty$  (*Model A*),  $\bar{m}_{\rho}=\infty$  (*Model B*), and  $\bar{m}_{\sigma,\rho}=\infty$  in *Model D*. For *Model C*, we take the same constraints as ref.[16], namely,  $g_{\sigma}=g_{\rho}$  and  $\bar{m}_{\sigma} = \bar{m}_{\rho}$ .

In the  $N/D$ -method, the full amplitude is written

$$a_{IJ} = \frac{N_{IJ}}{D_{IJ}}, \quad (3)$$

where  $N_{IJ}$  ( $D_{IJ}$ ) has a left- (right-) hand cut in the complex  $s$ -plane. The elastic unitarity implies  $\text{Im}D_{IJ}(s > 0) = -N_{IJ}$ . For the numerator function, we take  $N_{IJ}(s)=a_{IJ}^{\text{tree}}(s)$  together with  $D_{IJ}(0) = 1$ , which are consistent with the boundary condition  $a_{IJ}(s \rightarrow 0) \rightarrow b_{IJ}s$  obtained from chiral symmetry. Then the dispersion relation for  $D_{IJ}(s)$  reads

$$D_{IJ}(s) = \frac{1}{\pi} \int_0^{\infty} ds' \frac{-a_{IJ}^{\text{tree}}(s')}{s' - s - i\epsilon} + (\text{subtraction}). \quad (4)$$

Since  $a_{IJ}^{\text{tree}}(s \rightarrow \infty) \propto s$ , two subtractions are necessary to make  $D_{IJ}(s)$  finite. Namely two unknown parameters appear. One of them can be fixed by  $D_{IJ}(0) = 1$  mentioned above. Another one, which is written as  $d'_{IJ}(\mu)$  below, should be determined empirically at some energy scale  $\mu$ . Thus the final form of the denominator function reads

$$D_{IJ}(s) = 1 - d'_{IJ}(\mu)s + \frac{1}{\pi} \left( b_{IJ}s \ln \frac{-s}{\mu^2} - \sum_{\alpha=\sigma,\rho} b'_{\alpha IJ} d_{\alpha}(s/\bar{m}_{\alpha}^2) \right). \quad (5)$$

Here  $d_{\alpha}(x)$  is obtained by the dispersion integral of  $f_{\alpha}(x)$  in (1). Note that  $D_{IJ}(s)$  is  $\mu$  independent as a whole.

For our purpose, we need (i) to find complex poles of  $a_{IJ}(s)$  (or equivalently the complex zeros of  $D_{IJ}(s)$ ) in the 2nd Riemann sheet of the  $s$ -plane, and (ii) to find trajectories of those poles as a function of  $f_{\pi}^*$ . In eq.(5),

TABLE I: The bare mass  $\bar{m}_{\alpha}$  and  $d'_{11}$  extracted from the global fit of the phase shift in the  $I=J=1$  channel up to 1 GeV [24]. For *Model D*, we use  $L_1^r(\mu) = 0.4 \times 10^{-3}$  and  $L_2^r(\mu) = 1.4 \times 10^{-3}$  [26] to extract  $d'_{IJ}$  at  $\mu = 0.77$  GeV.  $d'_{00}$  obtained from  $d'_{11}$  is also shown.

Model	$\bar{m}_{\alpha}$ (GeV)	$d'_{11}$ (GeV <sup>-2</sup> )	$d'_{00}$ (GeV <sup>-2</sup> )
A	$\bar{m}_{\rho}=0.774$	-0.385	0.171
B	$\bar{m}_{\sigma}=0.838$	1.66	-3.04
C	$\bar{m}_{\rho,\sigma}=0.778$	-0.342	-0.0855
D	-	0.277	2.19

$\log(-z)$  and  $d_{\alpha}(z)$  have multi-valued structure.  $d_{\alpha}(z)$  contains both  $\ln(-z)$  and the Spence function  $\text{Sp}(z) = -\int_0^z dy \ln(1-y)/y$  [16]. The former (latter) has a branch cut along the real axis for  $\text{Re}z \geq 0$  ( $\text{Re}z \geq 1$ ). Then the analytic continuation of the Spence function to the 2nd sheet reads,

$$\text{Sp}^{\text{II}}(z) = \text{Sp}^{\text{I}}(z) + 2\pi i \cdot \text{Ln}(z), \quad (6)$$

where  $z$  is located in the lower half plane and  $\text{Ln}(z) \equiv \ln|z| + i\theta$  ( $-\pi < \theta \leq \pi$ ). The superscript I (II) indicates the 1st (2nd) sheet [23].

Here we mention briefly the determination of the unknown parameters ( $d'_{IJ}$ ,  $g_{\alpha}$  and  $\bar{m}_{\alpha}$ ) in each model. In *Models A, B* and *C*,  $g_{\rho}$  is fixed to be  $g_{\rho}^2/4\pi = 2.72$  for reproducing the  $\rho$ -width. In *Model B* and *C*,  $g_{\sigma}$  is assumed to be the same as  $g_{\rho}$  following Ref. [16]. Remaining parameters  $d'_{11}$  and  $\bar{m}_{\alpha}$  are adjusted by making a global fit to the experimental phase shift in the  $I=J=1$  channel up to 1 GeV [24]. Then,  $d'_{00}$  and  $d'_{20}$  are determined uniquely from  $d'_{11}$  by the constraints obtained from the matching to the  $O(p^4)$  chiral lagrangian for small  $s$  [16, 25]. For *Model D*,  $d_{IJ}$  is directly extracted from the coefficients  $L_{1,2}^r(\mu)$  in the  $O(p^4)$  chiral lagrangian. The  $I=J=1$  phase shift is not reproduced in *Model D*, since only  $\mathcal{L}_2$  is considered [21]. The results are listed in TABLE I for each model. We take the standard choice  $\mu=0.77$  GeV in determining the parameters. We have checked that the experimental phase shift in the  $(I,J)=(0,0)$  and  $(I,J)=(2,0)$  channels is reproduced quite well within the experimental error-bars in *Model B* and *C* below 0.9 GeV. *Model A* and *D* also show a qualitatively reasonable fit in the above channels at low energies. However, *Model A* underestimates attraction for  $(I,J)=(0,0)$  above 0.6 GeV. Also, *Model D* overestimates the attraction and repulsion above 0.4 GeV for  $(I,J)=(0,0)$  and  $(I,J)=(2,0)$ , respectively.

Before making numerical analysis of  $D_{IJ}(s)=0$ , let us first discuss its solution for small values of  $s$  where eq.(5) may be approximated as

$$D_{IJ}(s) \simeq 1 + (b_{IJ}/\pi)s \ln(-s/M^2), \quad (7)$$

in all four models. Here we have neglected  $O(s^{n \geq 2})$  terms and  $M$  is a  $\mu$ -independent scale defined as  $M^2 \equiv \mu^2 e^{d'(\mu)\pi/b}$ . Then a solution on the 2nd Riemann sheet

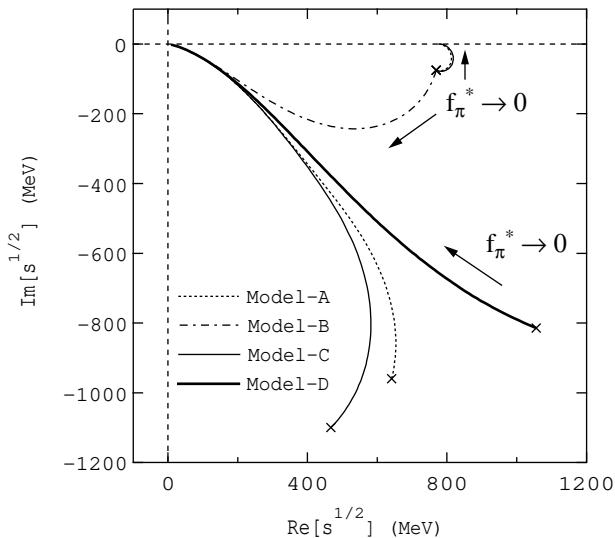


FIG. 1: The shift of the pole position in the  $I=J=1$  channel associated with the decrease of  $f_\pi^*$ . Two kinds of flows exist: one toward the origin and the other toward  $\bar{m}_\rho$  on the real axis. Crosses are the pole positions in the vacuum.

in  $(I,J)=(0,0), (1,1)$  channels reads

$$s_{IJ} = -(\pi/b_{IJ}) \cdot [W_{-1}(\pi/b_{IJ}M^2)]^{-1} \quad (8)$$

$$\rightarrow \frac{-F_{IJ}^{*2}}{\text{Ln}[-(F_{IJ}^{*2}/M^2)/\text{Ln}(F_{IJ}^{*2}/M^2)] - i\pi}, \quad (9)$$

where  $W_{-1}(z)$  is the  $(-1)$ -th branch of the Lambert  $W$  function [27]. From eq.(8) to eq.(9), we have used an asymptotic expansion of  $W_{-1}(z)$  valid for small and positive  $z$  [28]. Also,  $F_{00}^* = 4\pi f_\pi^*$  and  $F_{11}^* = \sqrt{6}F_{00}^*$ . Eq.(9) explicitly shows that resonance poles appear both in the  $\rho$  and the  $\sigma$  channels, and are softened *in tandem* as  $f_\pi^*$  decreases in nuclear medium.

For  $f_\pi^* \sim f_\pi$ , the small  $s$  approximation cannot be justified and more complicated behavior of the poles arises. To keep track of the trajectory of the poles for wide range of  $f_\pi^*$ , we show numerical solutions of eq.(5) for the  $I=J=1$  channel (Fig. 1) and for the  $I=J=0$  channel (Fig. 2). In these figures, the crosses indicate the position of the poles in the vacuum ( $f_\pi^*=f_\pi$ ). A common feature in *Models A, B and C* in the vacuum is that there always exists a narrow  $\rho$  ( $\sqrt{s_\rho} \simeq 769 - 76i$  MeV) and a broad/low-mass  $\sigma$ , no matter whether bare resonance are introduced or not. This is a kind of bootstrap situation discussed in [19]. Note also that, when the bare resonance is introduced, two complex poles appear as a result of an interplay between the bare resonance and the dynamically generated one. This can be seen in Fig. 1 for *Models A and C*, and in Fig. 2 for *Models B and C*. In *Model D* where bare resonances are not introduced, a broad and low-mass  $\sigma$  is dynamically generated while narrow  $\rho$  does not appear.

As  $f_\pi^*$  decreases from its vacuum value, we find two

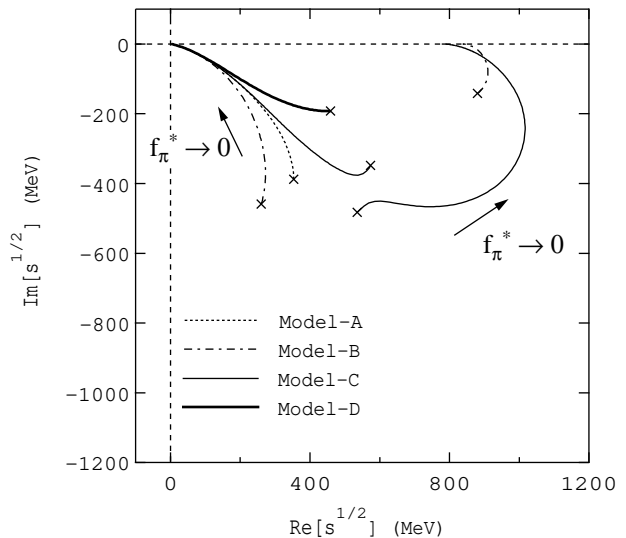


FIG. 2: The shift of the pole position in the  $I=J=0$  channel associated with the decrease of  $f_\pi^*$ . Two kinds of flows exist: one toward the origin and the other toward  $\bar{m}_\sigma$  on the real axis. Crosses are the pole positions in the vacuum.

types of trajectories in Figs. 1-2; those moving toward the origin and those moving toward  $\bar{m}_{\rho(\sigma)}$  on the real axis. The former trajectories in  $I=J=1$  and  $I=J=0$  channels are model independent and correspond to the universal softening evaluated in Eq.(9). Since the  $\pi$ - $\pi$  scattering amplitude is mainly affected by the poles close to the real axis, such soft mode gives a dominant contribution to the low-energy amplitude for  $f_\pi^*/f_\pi \ll 1$ .

On the other hand, when the system is close to the vacuum state ( $f_\pi^*/f_\pi \sim 1$ ), the above universality between  $\rho$  and  $\sigma$  breaks down. In fact, in the  $I=J=1$  channel, the narrow  $\rho$  resonance plays a dominant role and would-be soft mode is far away from the real-axis. In the  $I=J=0$  channel, on the contrary, the broad and low-mass  $\sigma$  keeps playing a role of the soft mode all the time.

The similarity and difference between the two channels for different values of  $f_\pi^*$  can be seen also by comparing the in-medium  $\pi$ - $\pi$  cross section calculated from  $a_{IJ}(s)$ .

The upper panel of Fig.3 (Fig.4) represents the in-medium cross section in *Model B* for  $0.5f_\pi \leq f_\pi^* \leq f_\pi$  in the  $I=J=1$  ( $I=J=0$ ) channel. We find that there is a moderate softening + broadening of the  $\rho$ -resonance at  $f_\pi^* = 0.7f_\pi$ , which is itself an interesting behavior in relation to the dilepton data in [4, 6]. However, even more significant change can be seen for the  $\sigma$ -resonance at the same value of  $f_\pi^*$ .

The lower panel of Fig.3 (Fig.4) represents the in-medium cross section in *Model B* for  $0.1f_\pi \leq f_\pi^* \leq 0.5f_\pi$  in the  $I=J=1$  ( $I=J=0$ ) channel. We find that sharp peaks develop in both channels as  $f_\pi^* \rightarrow 0$ . They are the direct consequence of the soft modes located near the origin for small  $f_\pi^*$  in Figs. 1-2. Namely, both  $I=J=1$  and  $I=J=0$  channels are good probes of chiral restoration in

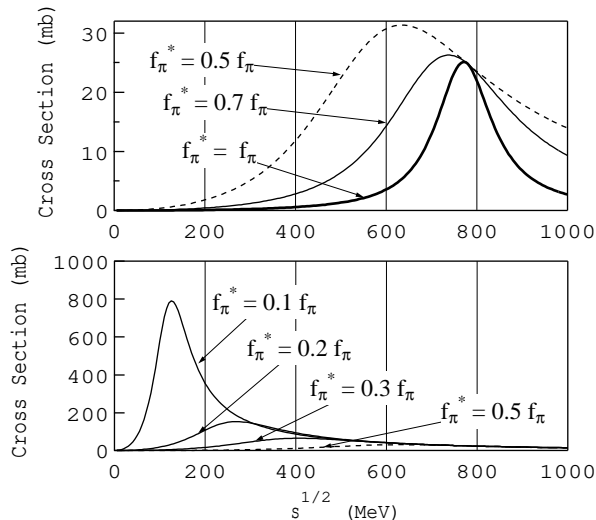


FIG. 3: The in-medium  $\pi$ - $\pi$  cross section in the  $I=J=1$  channel for *Model-B*. The upper (lower) panel shows the case for  $0.5f_\pi \leq f_\pi^* \leq f_\pi$  ( $0.1f_\pi \leq f_\pi^* \leq 0.5f_\pi$ ).

the medium if the chiral restoration is substantial. Although we have taken *Model B* as an example in Fig.3-4, we have checked that qualitative conclusions are the same for other models.

In summary, we have studied complex poles of the in-medium  $\pi$ - $\pi$  scattering amplitude in the  $I=J=0$  and  $I=J=1$  channels to explore possible relations between  $\sigma$  and  $\rho$  in nuclear matter. The  $N/D$  method is applied to four types of chiral models and the chiral restoration is modeled by the decrease of  $f_\pi^*$ . We have found universal complex poles in both channels moving in tandem toward the origin if  $f_\pi^*$  is sufficiently small. On the other

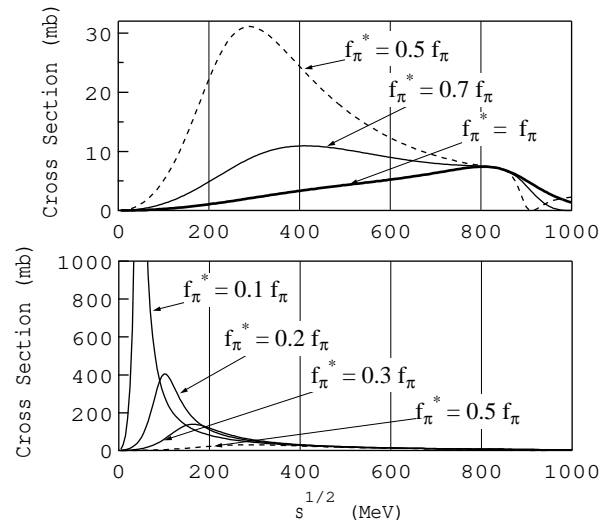


FIG. 4: Same with Fig. 3 for the  $I=J=0$  channel for *Model-B*.

hand, if  $f_\pi^*$  is not far from its vacuum value, interesting non-universal behavior arises and the two resonances act rather differently.

Inclusion of the finite pion mass, the medium effect beyond the mean-field approximation (such as the coupling to the particle-hole excitations of the Fermi-sea and the difference of  $f_{\pi,t}^*$  and  $f_{\pi,s}^*$  mentioned before) are future problems to be examined. Possible connection to other theoretical approaches [29] should be also studied.

This work is partially supported by the Grants-in-Aid of the Japanese Ministry of Education, Science and Culture (No. 12640263 and 12640296). A.H. is supported by JSPS Research Fellowship for Young Scientists.

- 
- [1] T. Hatsuda and T. Kunihiro, Phys. Rep. **247**, 221 (1994). G. E. Brown and M. Rho, Phys. Rep. **269**, 333 (1996).
- [2] R. D. Pisarski, Phys. Lett. **B110**, 155 (1982). G. E. Brown and M. Rho, Phys. Rev. Lett. **66**, 2720 (1991). T. Hatsuda and S. H. Lee, Phys. Rev. **C46**, R34 (1992). C. A. Dominguez and M. Loewe, Z. Phys. **C49**, 423 (1991). M. Asakawa, C.M. Ko, P. Levai, X.J. Qiu, Phys. Rev. **C46**, 1159 (1992). M. Herrmann, B.L. Friman, W. Norenberg, Nucl. Phys. **A560**, 411 (1993). C. A. Dominguez, M. Loewe and J. C. Rojas, Z. Phys. **C59**, 63 (1993).
- [3] T. Hatsuda and T. Kunihiro, Phys. Rev. Lett. **55**, 158 (1985); Phys. Lett. **B185**, 304 (1987). H. A. Weldon, Phys.Lett. **B274**,:133 (1992). S. Chiku and T. Hatsuda, Phys. Rev. **D58**, 076001 (1998). M.K. Volkov, E.A. Kuraev, D. Blaschke, G. Ropke and S.M. Schmidt, Phys. Lett. **B424**, 235 (1998). A. Patkos, Z. Szep and P. Szepfalusy, Phys. Lett. **B537** 77 (2002).
- [4] G. Agakishiev *et al.* (CERES/NA45 Collaboration), Phys. Lett. **B422**, 405 (1998).
- [5] See a review, R. Rapp and J. Wambach, Adv. Nucl. Phys. **25**, 1 (2000).
- [6] K. Ozawa *et al.* (E325 Collaboration), Phys. Rev. Lett. **86**, 5019 (2001).
- [7] F. Bonutti *et al.* (CHAOS Collaboration), Nucl. Phys. **A677**, 123 (2000).
- [8] A. Starostin *et al.* (Crystal Ball Collaboration), Phys. Rev. Lett. **85**, 5539 (2000).
- [9] P. Camerini *et al.*, Phys. Rev. **C46**, 067601 (2001).
- [10] V. Metag, in [12].
- [11] T. Kunihiro, Prog. Theor. Phys. Supplement **120**, 75 (1995).
- [12] Proceedings of *IPN Orsay Workshop on Chiral Fluctuations in Hadronic Matter*, ed. Z. Aouissat *et al.*, (Paris, France, Sep. 26-28, 2001).
- [13] T. Hatsuda, T. Kunihiro and H. Shimizu, Phys. Rev. Lett. **82**, 2840 (1999). Z. Aouissat, G. Chanfray, P. Schuck and J. Wambach, Phys. Rev. **C61**, 012202(R) (2000). D. Davesne, Y. J. Zhang and G. Chanfray, Phys. Rev. **C62**, 024604 (2000). However, see also, M. J. Vicente Vacas and E. Oset, nucl-th/0112048, nucl-th/0204055.

- [14] D. Jido, T. Hatsuda and T. Kunihiro, Phys. Rev. **D63**, 011901 (2001). T. Hatsuda and T. Kunihiro, nucl-th/0112027 in [12].
- [15] K. Nishijima, *Fields and Particles*, (Benjamin, New York, 1969).
- [16] K. Igi and K. Hikasa, Phys. Rev. **D59**, 034005 (1999).
- [17] J. A. Oller and E. Oset, Phys. Rev. **D60**, 074023 (1999).
- [18] J. L. Basdevant and J. Zinn-Justin, Phys. Rev. **D3**, 1865 (1971).
- [19] J. L. Basdevant, in *Cargèse lectures in Physics, Vol. 5*, ed. D. Bessis, p.431, (Gordon and Breach, New York).
- [20] J. L. Basdevant and B. W. Lee, Phys. Rev. **D2**, 1680 (1970).
- [21] J. A. Oller, E. Oset and J. R. Peláez, Phys. Rev. **D59**, 074001 (1999). G. Colangelo, J. Gasser, H. Leutwyler, Nucl. Phys. **B603**, 125 (2001).
- [22] U. G. Meissner, J.A. Oller and A. Wirzba, Annals. Phys. **297**, 27 (2002). Hung-chong Kim, Phys. Rev. **C65**, 055201 (2002). W. Weise, Nucl. Phys. **A690**, 98 (2001). P. Kienle and T. Yamazaki, Phys. Lett. **B514**, 1 (2001). E. Friedman, Phys. Lett. **B524**, 87 (2002). C. Garcia-Rocio, J. Nieves and E. Oset, nucl-th/0202038.
- [23] We have used,  $\text{Sp}^1(x + i\epsilon) - \text{Sp}^1(x - i\epsilon) = 2\pi i \cdot \ln x$  (for  $x$  real with  $x > 1$ ).
- [24] S. D. Protopopescu *et al.*, Phys. Rev. **D7**, 1279 (1973). P. Estabrooks and A. D. Martin, Prog. Part. Nucl. Phys. **79**, 301 (1974).
- [25]  $d'_{00}/4 = -d'_{11}/9 = -d'_{20}/4$  (*Model A*),  $d'_{00}/11 = -d'_{11}/6 = d'_{20}$  (*Model B*), and  $4d'_{00} = d'_{11} = d'_{20}$  (*Model C*) are obtained from the chiral constraint at  $O(p^4)$ . The results for *Model A* and *C* are consistent with those in [16].
- [26] G. Ecker, hep-ph/0011026.
- [27]  $W_k(z)$  is a  $k$ -th branch of the Lambert  $W$  function defined as the solution of  $W(z)e^{W(z)} = z$ . R. M. Corless *et al.*, Adv. Comp. Math. **5**, 329 (1996).
- [28] An asymptotic expansion for  $z \rightarrow 0, \infty$  reads  $W_{k \neq 0}(z) \simeq (\text{Ln}(z) + 2\pi ki) - \text{Ln}(\text{Ln}(z) + 2\pi ki) + \dots$  [27]. For real and positive  $z$ , one further finds  $W_{-1}(z \rightarrow 0) \simeq \text{Ln}(-z/\text{Ln}(z)) - i\pi + O(\pi/\text{Ln}(z), \text{Ln}(-\text{Ln}(z))/\text{Ln}(z))$ .
- [29] M. F. M. Lutz, G. Wolf and B. Friman, Nucl. Phys. **A706**, 431 (2002). M. Harada, Y. Kim and M. Rho, hep-ph/0111120.